

Research Article

Performance of sea water supported Pt–Sn–Mg/C catalyst for membraneless fuel cells

S. P. R. Kalaikathir, S. Begila David

Department of Chemistry, Women's Christian College, Nagercoli – 629 003, India.

Corresponding author e-mail: beginlas6@gmail.com

Abstract

The present work reports the performance of Pt–Sn–Mg/C ternary electrocatalysts on ethanol oxidation reaction in membraneless fuel cells prepared by thermal reduction method. A systematic investigation of ethanol adsorption and oxidation on binary and ternary electrocatalysts in sea water was performed in membraneless ethanol fuel cells. The different nominal compositions of binary Pt–Sn/C, Pt–Mg/C, and ternary Pt–Sn–Mg/C electrocatalysts were characterized by XRD, EDX, and TEM techniques. XRD and EDX confirmed the formation of Pt–Sn–Mg/C, Pt–Sn/C, and Pt–Mg/C metal catalyst with a typical Pt crystalline structure and the formation of Pt–Sn alloy. Electrochemical analyses obtained at room temperature by cyclic voltammetry and chronoamperometry showed that Pt₅₀Sn₄₀Mg₁₀/C gives a greater current density in comparison to that of Pt₅₀Sn₃₀Mg₂₀/C, Pt₅₀Sn₂₅Mg₂₅/C, Pt₅₀Sn₅₀/C, and Pt₅₀Mg₅₀/C. The power density obtained using Pt₅₀Sn₄₀Mg₁₀/C (39.2 mW cm⁻²) as an anode catalyst in membraneless ethanol fuel cell was higher than that using Pt₅₀Sn₃₀Mg₂₀/C, Pt₅₀Sn₂₅Mg₂₅/C, Pt₅₀Sn₅₀/C, and Pt₅₀Mg₅₀/C at the room temperature. CO poisoning can be reduced as a result of enhanced cell performance by the addition of Mg on the anode electrocatalysts. In this study, the carbon-supported binary Pt–Sn, Pt–Mg, and ternary Pt–Sn–Mg anode catalysts were successfully tested in a single membraneless fuel cell using 1.0 M ethanol and 0.5 M H₂SO₄ as the fuel and 0.1 M sodium perborate in sea water as the oxidant.

Keywords: Membraneless fuel cell; Electrocatalysts; Cyclic voltammetry; Chronoamperometry.

Introduction

The choice of sea water electrolyte is superior to facilitate the fuel cell development, make as the practice more efficient for fuel cell technologies. See water as electrolyte for membraneless ethanol fuel cell (MLEFC) enhances the hydrogen production during the electrochemical reaction. The use of ethanol as a fuel in membraneless ethanol fuel cell (MLEFC) has several advantages compared to that of hydrogen such as transport and storage, ease of handling and low operating temperature, and a high energy density [1-3].

Platinum was initially used as an electrocatalyst in the anode, as it was known to be the best electrocatalyst for the electro-oxidation of ethanol. However, the use of platinum is limited due to the CO poisoning effect; therefore, the use of binary electrocatalysts, where a new metal is added onto the Pt-base, has been studied [4-6]. It is

well known that the addition of Ru to Pt-based electrocatalysts lowers the over potential for the ethanol electro-oxidation reaction via a so-called bifunctional mechanism [7-9].

To further increase the catalytic activity of the anode, the introduction of a third metal to Pt–Sn/C binary catalyst was found to be the best electrocatalyst, because of its more tolerance to CO poisoning. Therefore, new alternative materials for electrocatalysts are required to minimize the noble metal loading and to optimum the catalytic performance. In this regard, many authors have intensively investigated Pt-based binary and ternary compounds to improve the performance of the electrocatalysts for the electrooxidation of ethanol [10-14]. Hence, we prepared Pt–Sn–Mg/C ternary alloy electrocatalysts by using thermal reduction method.

The enhanced activity of the ternary catalyst is due to the promoting effect of the second or

third elements added to Pt. In the present study, we evaluated the catalytic activity for ethanol oxidation reaction (EOR) by incorporating Co to Pt–Sn/C catalysts in MLEFC

Materials and methods

Materials

The metal precursors used for the preparation of electrocatalysts were $\text{H}_2\text{PtCl}_6 \cdot 6\text{H}_2\text{O}$ (from Sigma Aldrich), $\text{SnCl}_2 \cdot 3\text{H}_2\text{O}$ (from Sigma Aldrich) and $\text{MgSO}_4 \cdot 7\text{H}_2\text{O}$ (from Sigma Aldrich). Vulcan XC-72R carbon black (from Cabot Corp.) was used as a support for the catalysts. Graphite plates (from E-TEK) were used as substrates for the catalyst to prepare the electrodes. Nafion[®] (DE 521, DuPont USA) dispersion was used to make the catalyst slurry. Isopropyl alcohol (from Merck) was used as a solvent and NaBH_4 (from Merck) was used as the reduction agent. Ethanol (from Merck), sodium perborate (from Riedel) and H_2SO_4 (from Merck) and sea water were used as the fuel, the oxidant and as the electrolyte for electrochemical analysis, respectively. All the chemicals were of analytical grade. Pt/C (40-wt%, from E-TEK) was used as the cathode catalyst.

Catalyst preparation

Carbon supported ternary Pt–Sn–Mg catalysts with different atomic ratios were synthesized by thermal reduction method [15]. The carbon black was ultrasonically dispersed in a mixture of ultrapure water (Millipore MilliQ, 18 M Ω cm), and isopropyl alcohol for 20 min. Then the precursors were added to the ink, and then mixed thoroughly for 20 min. The ink was dried with a magnetic stirrer at 60°C. The dried $\text{H}_2\text{PtCl}_6 \cdot 6\text{H}_2\text{O}$, $\text{SnCl}_2 \cdot 3\text{H}_2\text{O}$ and $\text{MgSO}_4 \cdot 7\text{H}_2\text{O}$ compounds with carbon were put into a tube furnace and reduced at 400 °C with a gaseous mixture of H_2 and Ar with an atomic ratio of 1:9. The catalyst powder was stored in a vacuum vessel. For comparison, the monometallic Pt/C, bimetallic Pt–Sn/C and Pt–Mg/C catalysts were synthesized under the same conditions. The electrocatalytic mixtures and atomic ratios were Pt₅₀Sn₄₀Mg₁₀/C, Pt₅₀Sn₃₀Mg₂₀/C, Pt₅₀Sn₂₅Mg₂₅/C, Pt₅₀Sn₅₀/C, Pt₅₀Mg₅₀/C and Pt₁₀₀/C. The nominal loading of metals in the electrocatalysts was 40 % wt and rest 60 % wt was carbon.

Physical characterization

The morphology of the dispersed catalysts was examined using TEM (Philips CM 12 Transmission Electron Microscope). The particle size distribution and mean particle size were also evaluated using TEM. The crystal structure of the synthesized electrocatalysts was characterized by powder X-ray diffraction (XRD) using a Rigaku multiflex diffractometer (model RU-200 B) with $\text{Cu-K}\alpha_1$ radiation source ($\lambda_{\text{K}\alpha_1} = 1.5406 \text{ \AA}$) operating at room temperature. The tube current was 40 mA with a tube voltage of 40 kV. The 2θ angular regions between 20° and 90° were recorded at a scan rate of 5° min⁻¹. The mean particle size analyzed from TEM is verified by determining the crystallite size from XRD pattern using Scherrer formula. Pt (2 2 0) diffraction peak was selected to calculate crystallite size and lattice parameter of platinum. According to Scherrer's equation 1 [16].

$$d = \frac{0.9\lambda_{\text{K}\alpha_1}}{\beta_{2\theta} \cos \theta_{\max}} \quad (1)$$

where d is the average crystallite size, θ_{\max} is the angle at the position of the peak maximum, $\beta_{2\theta}$ is the width of the peak (in radians), 0.9 is the shape factor for spherical crystallite and $\lambda_{\text{K}\alpha_1}$ is the wavelength of X-rays used. The lattice parameters of the catalysts were estimated according to equation 2 [16].

$$a = \frac{\sqrt{2} \lambda_{\text{K}\alpha_1}}{\sin \theta_{\max}} \quad (2)$$

where a, is the lattice parameter (nm) and all the other symbols have the same meanings as in equation 1 [17]. The atomic ratio of the catalysts was determined by an energy dispersive X-ray (EDX) analyzer, which was integrated with the TEM instrument.

Electrochemical measurement

Electrochemical studies of the electrocatalysts were carried out using the thin porous coating technique. All electrochemical measurements were performed on an electrochemical workstation (CH Instruments, model CHI6650, USA) interfaced with a personal computer using the CHI software, at room temperature. A common three-electrode electrochemical cell using cyclic voltammetry (CV) and chronoamperometry (CA) techniques was used for the measurements. Catalyst coated

glassy carbon electrode (GCE, 3 mm diameter and 0.071 cm² of electrode area, from CHI, USA) was used as the working electrode and platinum foil was used as the counter electrode. Ag/AgCl in saturated KCl was used as the reference electrode (RHE). The working electrode was prepared by applying catalyst ink made of 20 mg of electrocatalyst in a solution of 50 mL of water containing three drops of 6% PTFE suspension. The resulting mixture was treated in an ultrasound bath for 10 min to obtain a uniform dispersion. The catalyst slurry was then drop-cast on to a glassy carbon electrode and allowed to dry at 100 °C for 30 min. For assessing the electrocatalytic activity of the working electrode, cyclic voltammetry was obtained in 1.0 M ethanol and 0.5 M H₂SO₄ solution with a scan rate of 50 mV s⁻¹. For the durability test, the chronoamperometric experiments were carried out at 0.1 V for 2500 s in the same electrolyte. Before each measurement, the solution was purged with high-purity nitrogen gas for at least 30 min to ensure oxygen-free measurements.

Single cell test

In the present study, we fabricated the membraneless ethanol fuel cell (MLEFC) using laminar flow-based fuel cell configuration [18]. In this membraneless fuel cell, ethanol is used as a fuel, sodium perborate is used as an oxidant and sea water is used as an electrolyte. In membraneless fuel cell system sea water used as electrolyte for more accurate that allows both high energy density and low environmental impact at a low cost. In crystalline state sodium perborate exist as a dimeric peroxy-salt with water of hydration, but in aqueous solution affords hydrogen peroxide as shown in Eq. (3),

$$[\text{B}(\text{OH})_3(\text{O}_2\text{H})]^- + \text{H}_2\text{O} \rightleftharpoons [\text{B}(\text{OH})_4]^- + \text{H}_2\text{O}_2 \quad (3)$$

In MLEFC, the aqueous fuel and oxidant streams flow in parallel in a single microchannel with the anode and cathode on opposing sidewalls (Fig. 1). Graphite plates of one mm thickness served as current collectors and catalyst support structures. The different anode and cathode catalysts were coated onto the graphite plates. For single cell, the anode catalysts with different atomic ratios were prepared as follows: The catalyst ink was prepared by mixing required quantity of catalyst with a solution of 50 mL of water containing three drops of 6% PTFE dispersion in an

ultrasonic bath for 10 min to obtain a uniform dispersion. The catalyst slurry was then spread on the graphite plate by brush and dried at 100 °C for 30 min to obtain anode and cathode electrodes. The catalysts tested on the anode side were Pt₅₀Sn₄₀Mg₁₀/C, Pt₅₀Sn₃₀Mg₂₀/C, Pt₅₀Sn₂₅Mg₂₅/C, Pt₅₀Sn₅₀/C, Pt₅₀Mg₅₀/C and Pt₁₀₀/C, Pt with catalyst loading 2 mg/cm². On the cathode side, Pt/C (100) with catalyst loading 2 mg/cm² was used in all experiments.

The two catalyst-coated graphite plates were aligned to form a channel with 0.1 cm electrode-to-electrode distance (width), a 3 cm length, and a 0.1 cm height. The anolyte (fuel and electrolyte) and catholyte (oxidant and sea water) streams flow in a laminar fashion over the anode and cathode, respectively. The electrode area along a microchannel wall between the inlets and the outlet (3 cm long and 0.1 cm wide) was used as the geometric surface area of the electrodes in this study (0.3 cm²). The design is described in detail elsewhere. The anolyte used in the anode side was 1.0 M ethanol + 0.5 M H₂SO₄ and the catholyte used in the cathode side was 0.1 M perborate in sea water. The flow rate of each of the streams was 0.3 mL min⁻¹ (total flow rate of 0.6 mL min⁻¹). The MLEFC was operated at room temperature. The current-voltage characteristics of MLEFC were measured using an electrochemical workstation (CH Instruments, model CHI6650, USA) and the data was verified using a multi-meter (MASTECH[®] MAS830L).

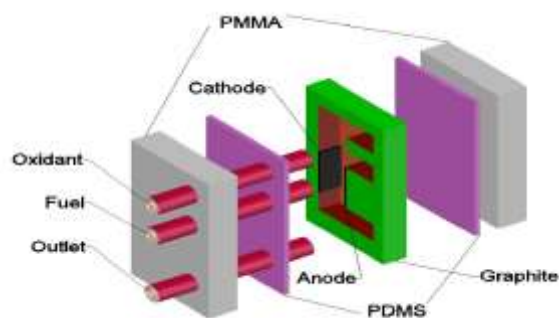


Fig. 1 Schematic of the E-shaped membraneless laminar flow based fuel cell with graphite plates molded with PDMS poly(dimethylsiloxane) and sealed with PMMA poly(methylmethacrylate).

Results and discussion

Physical Characterization

X-ray Diffraction (XRD)

The XRD patterns of the prepared Pt₅₀Sn₄₀Mg₁₀/C, Pt₅₀Sn₃₀Mg₂₀/C,

Pt₅₀Sn₂₅Mg₂₅/C, Pt₅₀Sn₅₀/C, Pt₅₀Mg₅₀/C and Pt₁₀₀/C, catalysts are shown in Fig. 2. The first peak located at around 25° in all the XRD patterns is attributable to the Vulcan XC-72R carbon support.

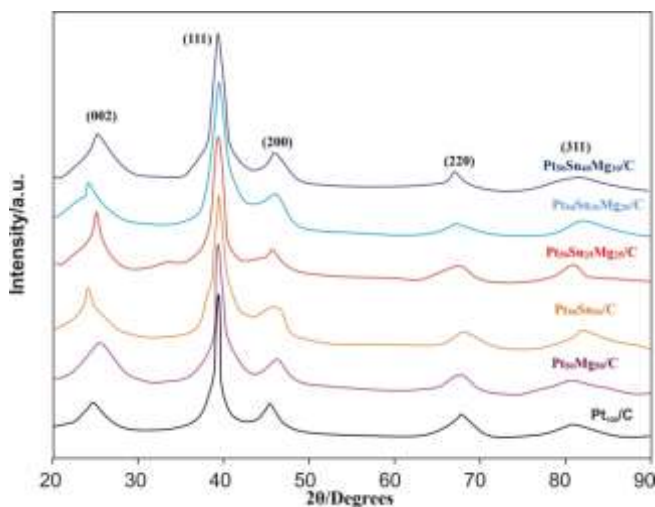


Fig. 2. X-ray diffraction patterns of Pt₅₀Sn₄₀Mg₁₀/C, Pt₅₀Sn₃₀Mg₂₀/C, Pt₅₀Sn₂₅Mg₂₅/C, Pt₅₀Sn₅₀/C, Pt₅₀Mg₅₀/C and Pt₁₀₀/C catalysts

The 2θ of the (2 2 0) peak for Pt₅₀Sn₄₀Mg₁₀/C, Pt₅₀Sn₃₀Mg₂₀/C, Pt₅₀Sn₂₅Mg₂₅/C, Pt₅₀Sn₅₀/C, and Pt₅₀Mg₅₀/C, shows a higher angle shift than the characteristics of face-centered cubic (fcc) crystalline Pt at 2θ values of

39°, 47°, 67° and 82° and are indexed with planes (1 1 1), (2 0 0), (2 2 0) and (3 1 1), respectively, indicating that the electrocatalysts have good alloy formations and suggesting the effect of a different atomic rate of Mg in the ternary catalyst. No diffraction peaks were attributed to pure tin and magnesium metals or tin rich hexagonal close packed (hcp) phase, appear in the XRD patterns, suggesting that tin and magnesium atoms either form an alloy with platinum or exist as amorphous oxide phases. The Pt–Mg/C electrocatalyst also showed the same characteristic peak as that of the Pt–Sn/C electrocatalysts.

The fcc lattice parameters were evaluated from the angular position of the (2 2 0) peaks, which reflect the formation of a solid solution (Table 1). The decrease in lattice parameters of the alloy catalysts reflects the progressive increase in the incorporation of Sn and Mg into the alloyed state. The difference of lattice parameters and the shift of (2 2 0) plane indicate interactions between Pt, Sn and Mg. The average particle size for Pt–Sn/C, Pt–Mg/C, and Pt–Sn–Mg/C electrocatalysts were in the range of 2.9–4.5 nm was estimated using the Scherrer equation in (1)

Table 1. The EDX composition, lattice parameters, and the particle size obtained for different atomic ratios of electrocatalysts

Electrocatalyst	Nominal Atomic ratio			EDX Atomic ratio			Lattice parameter	Crystallite size (nm)	Particle size from TEM (nm)
	Pt	Sn	Mg	Pt	Sn	Mg			
Pt/C	100	-	-	99	-	-	0.3915	4.3	4.0
Pt–Mg/C	50	-	50	52	-	48	0.3898	4.1	3.9
Pt–Sn/C	50	50	-	51	49	-	0.3905	3.6	3.3
Pt–Sn–Mg/C	50	25	25	51	25	24	0.3903	3.5	3.2
Pt–Sn–Mg/C	50	30	20	51	28	19	0.3897	3.4	3.2
Pt–Sn–Mg/C	50	40	10	52	38	11	0.3894	3.2	2.9

Transmission Electron Microscopy (TEM)

TEM image of the Pt₅₀Sn₄₀Mg₁₀/C, Pt₅₀Sn₃₀Mg₂₀/C and Pt₅₀Sn₂₅Mg₂₅/C alloy catalysts and the corresponding particle size distribution histogram are presented in Fig. 3. From the TEM images, the average particle diameter was found to be approximately 3–3.5 nm, which is in fairly good agreement with the data calculated from XRD. The particle size distribution of these catalysts is shown in Table 1 in accordance to the TEM images.

Energy Dispersive X-ray Spectroscopy (EDX)

Energy dispersive X-ray spectroscopy is conducted by focusing the electron beam on several different selected regions of the carbon supported Pt–Sn–Mg nanoparticles. An EDX spectrum of Pt–Sn–Mg/C nanoparticle is shown in Fig. 4. The average composition of the sample was in atom ratio of Pt:Sn:Mg = 5:4:1. The EDX results of the Pt/C, binary Pt–Sn/C and ternary Pt–Sn–Mg/C catalysts are very close to the nominal values, which indicate that the metals

were loaded onto the carbon support without

obvious loss.

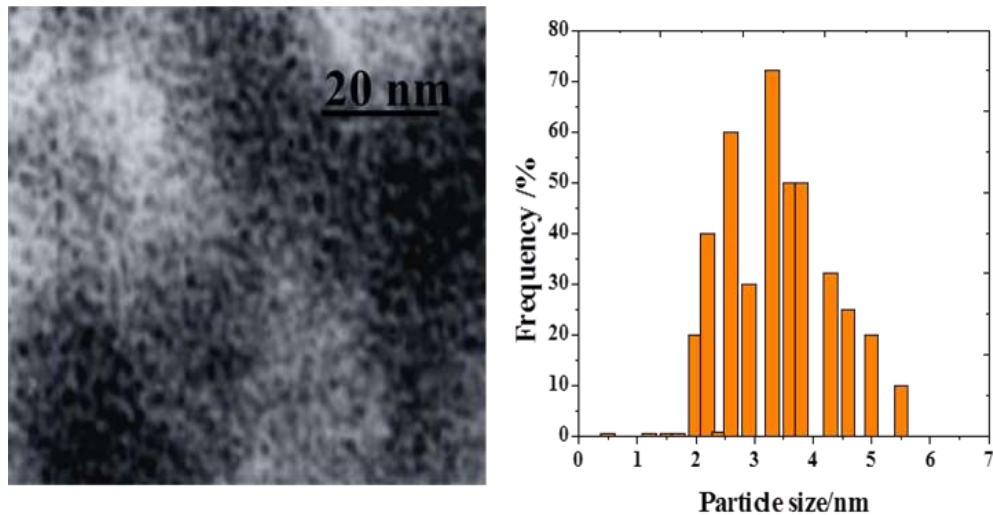


Fig. 3. TEM image and particle size distribution of a) Pt₅₀Sn₄₀Mg₁₀/C catalyst

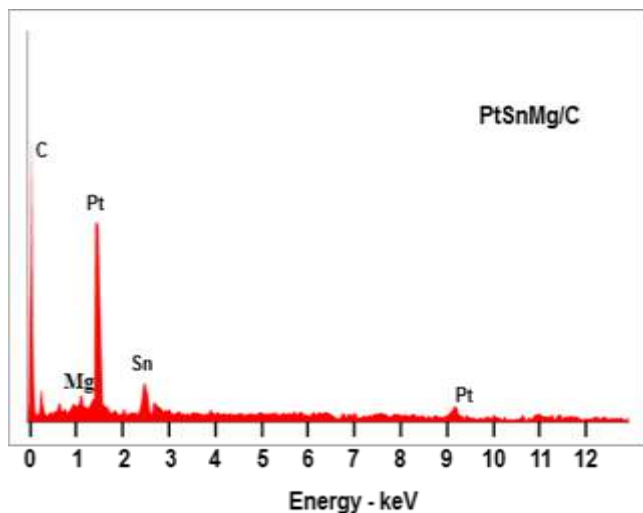


Fig. 4. EDX spectra of Pt–Sn–Mg/C catalysts

Electrochemical characterization

Cyclic voltammetry

Fig. 5(a) shows the cyclic voltammogram (CV) on the Pt₅₀Sn₄₀Mg₁₀/C, Pt₅₀Sn₃₀Mg₂₀/C, Pt₅₀Sn₂₅Mg₂₅/C, Pt₅₀Sn₅₀/C, Pt₅₀Mg₅₀/C and Pt₁₀₀/C catalysts for CO oxidation in a solution of 0.5 M H₂SO₄. Due to the strong adsorption of CO onto the Pt surface, the hydrogen adsorption-desorption of the Pt was completely blocked in the hydrogen region; indicating the presence of a saturated CO adlayer [19].

The electrochemically active surface areas (SEAS) of the electrocatalysts were calculated by using Eq. (4) [20-21]. S_{EAS} values were estimated using CO adsorption (S_{EAS/CO}) and roughness of electrodes.

$$S_{EAS/CO}(m^2/g) = \frac{Q_{CO}(\mu C/cm^2)}{420(\mu C/cm^2) \times [Pt]} \quad (4)$$

Where Q_{CO} is the charge corresponding to CO on the Pt surface, $[Pt]$ (mg/cm²) is the Pt loading on the electrode surface, 420 μC/real cm² is the charge required to oxidize a monolayer of CO on the Pt surface. The roughness of each electrode is calculated by dividing S_{EAS} obtained with the apparent surface area.

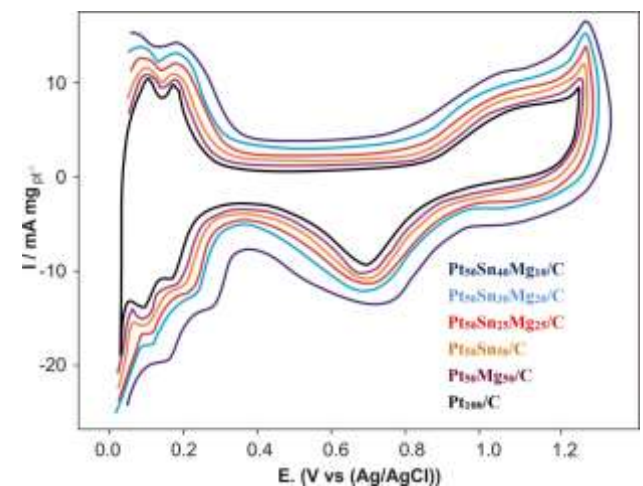


Fig. 5(a). CVs of Pt₅₀Sn₄₀Mg₁₀/C, Pt₅₀Sn₃₀Mg₂₀/C, Pt₅₀Sn₂₅Mg₂₅/C, Pt₅₀Sn₅₀/C, Pt₅₀Mg₅₀/C and Pt₁₀₀/C electrocatalysts in 0.5 M H₂SO₄

Estimation of the electrode roughness and S_{EAS} values are shown in Table 2. Based on these values, the highest electrochemically active area is achieved for the ternary electrocatalysts. The real surface area estimated by this method is in good agreement with the enhancement in electrocatalytic activity. It is shown that Mg-

modified Pt–Sn/C surfaces offer energetically different sites for adsorption and oxidative desorption, which can be selectively populated by CO species; either *via* the direct adsorption of

CO dissolved in the electrolyte or *via* the adsorption and decomposition reaction of ethanol.

Table 2. Comparison of hydrogen desorption charge and carbon monoxide desorption charge, and its electrochemical active surface area (S_{EAS}) and electrode roughness

Catalyst	$Q_{CO}/\mu C$	Electrode real Surface area (cm^2)	$S_{EAS/CO}$ (m^2gPt^{-1}) ^a	Roughness
Pt ₁₀₀ /C	1260	3.1	31	83.0
Pt ₅₀ Mg ₅₀ /C	672	1.5	33	43.8
Pt ₅₀ Sn ₅₀ /C	736	1.8	36	48.1
Pt ₅₀ Sn ₂₅ Mg ₂₅ /C	841	2.0	41	56.4
Pt ₅₀ Sn ₃₀ Mg ₂₀ /C	965	2.4	47	64.6
Pt ₅₀ Sn ₄₀ Mg ₁₀ /C	1025	2.5	48	68.8

The CV curves were obtained in a half cell between 0.05 and 1.2 V (*vs.* Ag/AgCl) in the absence of ethanol. The characteristic features of polycrystalline Pt, i.e. hydrogen adsorption/desorption peaks in low potential region, oxide formation/stripping wave/peak in high potential region and a flat double layer in between, are observed for all the synthesized catalysts. The voltammograms of the electrocatalysts did not display a well-defined hydrogen region between 0.05 and 0.35 V, as the catalyst's features in this region are influenced by their surface composition. Taking the Pt₁₀₀/C composition as a reference, the binary Pt₅₀Sn₅₀/C and Pt₅₀Mg₅₀/C catalysts showed a voltammetric charge similar to that of the pure Pt catalyst. However, a considerable increase in the voltammetric charge of ternary Pt₅₀Sn₄₀Mg₁₀/C catalyst was observed in the double-layer region, indicating that the addition of W into binary Pt–Sn/C leads to an enhanced activity for the oxidation reactions.

Fig. 5(b) corresponds to representative CVs of ethanol oxidation under acidic conditions (1.0 M CH₃CH₂OH and 0.5 M H₂SO₄) catalyzed by Pt₅₀Sn₄₀Mg₁₀/C, Pt₅₀Sn₃₀Mg₂₀/C, Pt₅₀Sn₂₅Mg₂₅/C, Pt₅₀Sn₅₀/C, Pt₅₀Mg₅₀/C and Pt₁₀₀/C catalysts. The onset potential for the oxidation of ethanol in a positive scan was a key factor for evaluating the catalyst activity. The onset potentials for the oxidation of ethanol on the Pt₅₀Sn₄₀Mg₁₀/C (0.31 V), Pt₅₀Sn₃₀Mg₂₀/C (0.35 V) and Pt₅₀Sn₂₅Mg₂₅/C (0.39 V) electrocatalysts were slightly lower than that on the Pt₅₀Sn₅₀/C (0.40 V), Pt₅₀Mg₅₀/C (0.43 V) and Pt₁₀₀/C (0.47 V) catalysts. All the current values were normalized by the geometric surface area of the electrode used. The CV curves depict the

presence of a peak in the potential range of the positive sweep and another peak in the negative sweep.

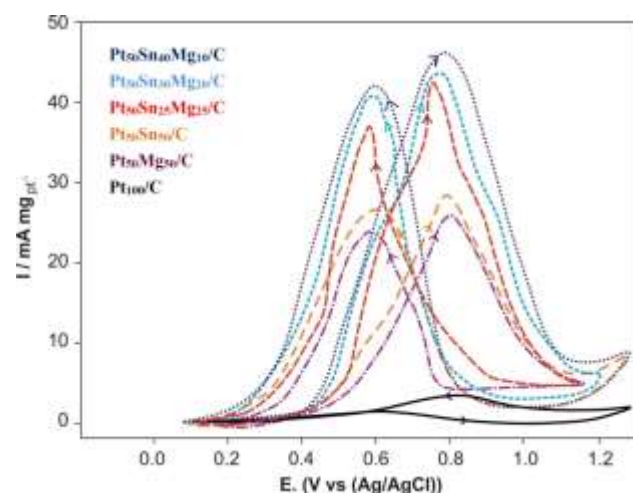


Fig. 5(b). CVs of Pt₅₀Sn₄₀Mg₁₀/C, Pt₅₀Sn₃₀Mg₂₀/C, Pt₅₀Sn₂₅Mg₂₅/C, Pt₅₀Sn₅₀/C, Pt₅₀Mg₅₀/C and Pt₁₀₀/C electrocatalysts in 1.0 M ethanol + 0.5 M H₂SO₄

The peak in the positive sweep is associated with the ethanol oxidation, and the peak in the negative sweep is related to the oxidation of carbonaceous intermediate products from incomplete ethanol oxidation. The peak current densities of Pt₅₀Sn₄₀Mg₁₀/C, Pt₅₀Sn₃₀Mg₂₀/C, Pt₅₀Sn₂₅Mg₂₅/C, Pt₅₀Sn₅₀/C, Pt₅₀Mg₅₀/C and Pt₁₀₀/C catalysts are 47.8, 42.8, 41.6, 25.8, 24.6 and 4.59 mA/cm², respectively, showing that the activity of the ternary Pt₅₀Sn₄₀Mg₁₀/C catalyst is a factor of ~9 times higher than that of the Pt/C catalyst. Table 3 summarizes the CV results of Pt₅₀Sn₄₀Mg₁₀/C, Pt₅₀Sn₃₀Mg₂₀/C, Pt₅₀Sn₂₅Mg₂₅/C, Pt₅₀Sn₅₀/C, Pt₅₀Mg₅₀/C and Pt₁₀₀/C electrocatalysts including the positive peak potentials and the corresponding peak current densities of EOR.

The CV results show that pure Pt₁₀₀/C catalysts do not behave as an appropriate anode for EOR due to its poisoning by strongly adsorbed intermediates such as CH₃COOH. However, the introduction of Sn and Mg promotes the electrocatalytic activity.

adsorbed intermediates such as CH₃COOH. However, the introduction of Sn and Mg promotes the electrocatalytic activity.

Table 3. CV results of Pt₅₀Sn₄₀Mg₁₀/C, Pt₅₀Sn₃₀Mg₂₀/C, Pt₅₀Sn₂₅Mg₂₅/C, Pt₅₀Sn₅₀/C, Pt₅₀Mg₅₀/C and Pt₁₀₀/C electrocatalysts

Catalyst	Scan rate 50 mV s ⁻¹	
	Positive peak potential (mV vs. Ag/AgCl)	/ Peak current density (mA/cm ²)
Pt ₁₀₀ /C	888	4.59
Pt ₅₀ Mg ₅₀ /C	876	24.6
Pt ₅₀ Sn ₅₀ /C	889	25.8
Pt ₅₀ Sn ₂₅ Mg ₂₅ /C	890	41.6
Pt ₅₀ Sn ₃₀ Mg ₂₀ /C	895	42.8
Pt ₅₀ Sn ₄₀ Mg ₁₀ /C	905	47.8

Chronoamperometry

Fig. 6 shows the current densities measured at a constant potential jumping from 0.05 to 1.2 V in 1.0 M ethanol+0.5 M H₂SO₄. The currents decay with time in a parabolic style and reach an apparent steady state within 80s. It can be seen that the current density of ethanol electrooxidation on the Pt₅₀Sn₄₀Mg₁₀/C catalyst is higher than that on the Pt₅₀Sn₃₀Mg₂₀/C, Pt₅₀Sn₂₅Mg₂₅/C, Pt₅₀Sn₅₀/C, Pt₅₀Mg₅₀/C and Pt₁₀₀/C catalyst at the same potentials. The activity change for ethanol oxidation decreases in the order of Pt₅₀Sn₄₀Mg₁₀/C > Pt₅₀Sn₃₀Mg₂₀/C > Pt₅₀Sn₂₅Mg₂₅/C > Pt₅₀Sn₅₀/C > Pt₅₀Mg₅₀/C > Pt₁₀₀/C, which is in fairly good agreement with our CV results.

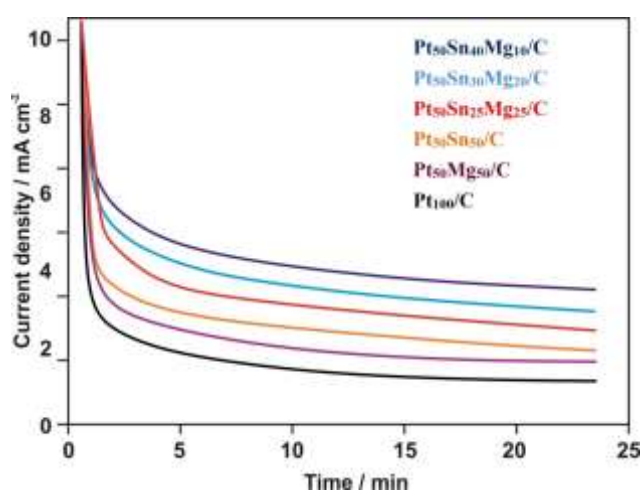


Fig. 6. CA of Pt₅₀Sn₄₀Mg₁₀/C, Pt₅₀Sn₃₀Mg₂₀/C, Pt₅₀Sn₂₅Mg₂₅/C, Pt₅₀Sn₅₀/C, Pt₅₀Mg₅₀/C and Pt₁₀₀/C electrocatalysts

For the durability test, the chronoamperometric experiments were carried out at 0.05 to 1.2 V for 25 min in the same conditions. Before each measurement, the solution was purged with high-purity nitrogen

gas for at least 30 min to ensure oxygen-free measurements.

Effect of sea water on single cell performance

The microfluidic architecture of laminar flow-based membraneless fuel cells overcomes the fuel crossover and water management issues that plague membrane-based fuel cells (i.e., PEMFC, DEFC) and enables independent control of stream characteristics (i.e., flow-rate and composition). Here we focused on maximizing cell performance, in terms of power density, by tailoring various structural characteristics and catalytic activity of carbon supported ternary Pt–Sn–W catalysts. A single cell performance was tested using Pt₅₀Sn₄₀Mg₁₀/C, Pt₅₀Sn₃₀Mg₂₀/C, Pt₅₀Sn₂₅Mg₂₅/C, Pt₅₀Sn₅₀/C, Pt₅₀Mg₅₀/C and Pt₁₀₀/C electrocatalysts as the anode. Polarization curves and power densities are shown in Fig. 7. For each catalyst, the open-circuit voltages (OCV) were different, as would be expected in onset potentials. The OCVs of Pt₅₀Sn₄₀Mg₁₀/C, Pt₅₀Sn₃₀Mg₂₀/C, Pt₅₀Sn₂₅Mg₂₅/C, Pt₅₀Sn₅₀/C, Pt₅₀Mg₅₀/C, are higher than that of Pt₁₀₀/C, 0.53 V, and the order of OCV is exactly same as the onset potentials.

The OCV of Pt₅₀Sn₄₀Mg₁₀/C is the highest value of 0.880 V, which is approximately 0.36 V higher than that of Pt₁₀₀/C. This indicates that Pt₁₀₀/C is more rapidly poisoned by CH₃COOH than any other alloy catalyst and that the oxidation of adsorbed CH₃COOH is enhanced by the second or third metal. In the case of Pt₅₀Sn₄₀Mg₁₀/C the overall performance is superior to that of the bimetallic electrocatalysts. The maximum power densities obtained for Pt₅₀Sn₄₀Mg₁₀/C, Pt₅₀Sn₃₀Mg₂₀/C, Pt₅₀Sn₂₅Mg₂₅/C, Pt₅₀Sn₅₀/C, Pt₅₀Mg₅₀/C and

Pt₁₀₀/C are 39.2, 36.7, 30.4, 29.0, 20.4 and 6.7 mW cm⁻², respectively (Table 4). We conclude that the substitution of a small amount of Mg for Sn and the electrogeneration of seawater aids in

cleaning surfaces poisoned by CO and CH₃COOH and provide additional reaction sites for ethanol oxidation.

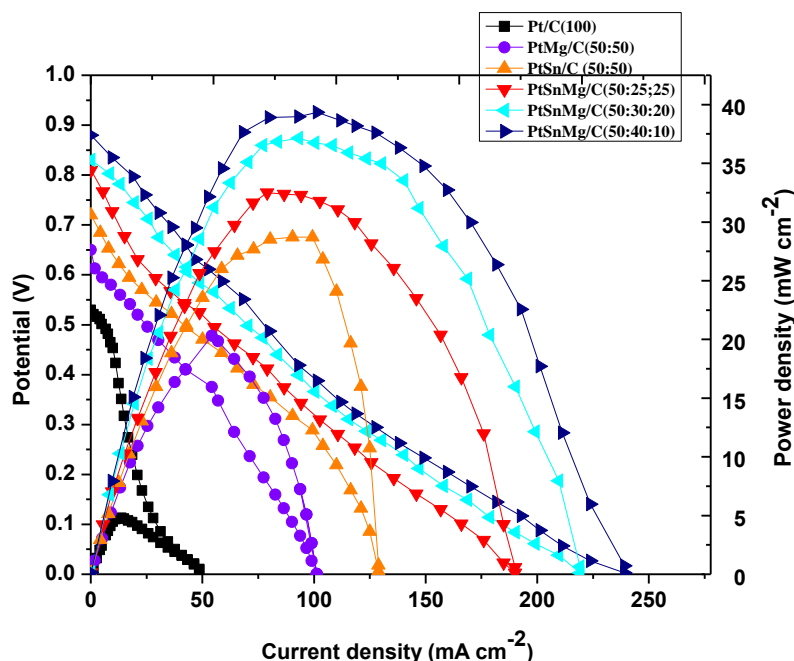


Fig. 7. Polarization and power density curves of Pt₅₀Sn₄₀Mg₁₀/C, Pt₅₀Sn₃₀Mg₂₀/C, Pt₅₀Sn₂₅Mg₂₅/C, Pt₅₀Sn₅₀/C, Pt₅₀Mg₅₀/C and Pt₁₀₀/C electrocatalysts

In membraneless fuel cells, pure Pt/C catalyst does not behave as a very good anode for ethanol electro-oxidation due to its poisoning by strongly adsorbed intermediates such as CO and CH₃COOH [22]. The binary and ternary electrocatalysts performed better than Pt/C for ethanol oxidation. Moreover, when the binary electrocatalysts were compared to the ternary ones in terms of oxidation the latter catalysts gave the best electrical performances. On the

other hand, addition of Mg to Pt (Pt–Mg/C) had a little effect, whereas addition of Mg to Pt–Sn greatly enhanced the electrocatalytic activity. As mentioned in our earlier studies [23] these results also demonstrated that the performance of the developed membraneless fuel cell enhanced profoundly if the concentration of oxidant in cathodic stream is 10 times larger, and the current density is also increased approximately ten times.

Table 4. Summary of performance of single fuel cell tests using (2 mg cm⁻² catalyst loading, 40 wt% catalyst on carbon)

Anode catalysts	Open circuit Voltage (V)	Maximum power density (mW cm ⁻²)	Maximum current density (mA cm ⁻²)
Pt ₁₀₀ /C	0.53	6.7	48.7
Pt ₅₀ Mg ₅₀ /C	0.65	20.4	100.1
Pt ₅₀ Sn ₅₀ /C	0.72	29.0	129.1
Pt ₅₀ Sn ₂₅ Mg ₂₅ /C	0.81	30.4	189.6
Pt ₅₀ Sn ₃₀ Mg ₂₀ /C	0.83	36.7	219.2
Pt ₅₀ Sn ₄₀ Mg ₁₀ /C	0.88	39.2	239.1

Conclusions

The present study of ethanol oxidation in presence of sea water on carbon-supported Pt–Sn–Mg ternary nanoparticles has revealed details concerning the activity and stability of the catalysts in membraneless fuel cells. The maximum activity for ethanol oxidation was

found for the Pt₅₀Sn₄₀Mg₁₀/C than the Pt₅₀Sn₃₀Mg₂₀/C, Pt₅₀Sn₂₅Mg₂₅/C, Pt₅₀Sn₅₀/C, Pt₅₀Mg₅₀/C and Pt₁₀₀/C. The significantly enhanced catalytic activity for ethanol oxidation can be attributed to the high dispersion of ternary catalysts and to Mg acting as a promoting agent along with the electrogeneration of seawater.

XRD results show the homogenous alloy structure of Pt, Sn and Mg. The TEM images indicated an average size of Pt₅₀Sn₄₀Mg₁₀/C, Pt₅₀Sn₃₀Mg₂₀/C and Pt₅₀Sn₂₅Mg₂₅/C nanoparticles of 3-3.5 nm. The atom ratio of Pt, Sn and Mg from EDX analyses is close agreement with the original precursor concentration. The composition of ternary Pt₅₀Sn₄₀Mg₁₀/C nanoparticles can be conveniently controlled by adjusting the initial metal salt solution and preparation conditions. The electrochemical experiments showed that the Pt₅₀Sn₄₀Mg₁₀/C nanoparticles have higher catalytic activity than that of the other catalysts in sea water electrolyte. It is also observed that the activity of electrocatalysts was diminished in the absence of sea water. We expect that the MLEFC may be a promising candidate for practical fuel cells to establish a clean and sustainable energy future. Further work is necessary to characterize the catalysts using different surface analysis techniques and to conduct tests of these electrocatalysts in microfluidic membraneless fuel cells in presence and absence of sea water.

Acknowledgments

The financial support for this research from University Grants Commission (UGC), New Delhi, and the presidency college department of chemistry are gratefully acknowledged.

Conflict of interest

Authors declare there are no conflicts of interest.

References

- [1] Ren X, Zelenay P, Thomas S, Davey J, Gottesfeld S. Recent advances in direct methanol fuel cells at los Alamos national laboratory. *J Power Sources*, 2000;86:111-116.
- [2] Choi WC, Woo SI. Bimetallic Pt-Ru nanowire network for anode material in a direct-methanol fuel cell. *J Power Sources*. 2003;124:420-425.
- [3] Yamaguchi T, Kuroki H, Miyata F. DMFC performances using a pore-filling polymer electrolyte membrane for portable usages. *Electrochem Commun*. 2005;7:730-734.
- [4] Xu J, Hua K, Sun G, Wang C, Lv X, Wang Y. Electrooxidation of methanol on carbon nanotubes supported Pt-Fe alloy electrode. *Electrochem Commun*. 2006;8:982-986.
- [5] Luo J, Njoki PN, Lin Y, Mott D, Wang L, Zhong C. Characterization of carbon-supported AuPt Nanoparticles for electrocatalytic methanol oxidation reaction. *Langmuir*. 2006;22:2892-2898.
- [6] Shobha T, Aravinda CL, Bera P, Devi LG, Mayanna SM. Characterization of Ni-Pd alloy as anode for methanol oxidative fuel cell. *Mater Chem Phys*. 2003;80:656-661.
- [7] Gasteiger HA, Markovic N, Ross PN, Cairns EJ, Methanol electrooxidation on well-characterized Pt-Ru alloys. *J Phys Chem*. 1993;97:12020-12029.
- [8] Markovic NM, Gasteiger HA, Ross PN, Jiang XD, Villegas I, Weaver MJ, Electro-oxidation mechanisms of methanol and formic acid on Pt-Ru alloy surfaces. *Electrochimica Acta*. 1995;40:91-98.
- [9] Yajima T, Uchida H, Watanabe M. In-Situ ATR-FTIR spectroscopy study of electro-oxidation of methanol and adsorbed CO at Pt-Ru alloy. *J Phys Chem B*. 2004;108:2654–2659.
- [10] Sivakumar P, Tricoli V, Pt-Ru-Ir nanoparticles prepared by vapour deposition as a very efficient anode catalyst for methanol fuel cells. *Electrochem Solid State Lett*. 2006;9:A167.
- [11] Neto AO, Dias RR, Tusi MM, Linardi M, Spinace EV, Electro-oxidation of methanol and ethanol using PtRu/C, PtSn/C and PtSnRu/C electrocatalysts prepared by an alcohol-reduction process. *J Power Sources*. 2007;166:87-91.
- [12] Wang ZB, Zuo PJ, Yin GP, Effect of W on activity of Pt-Ru/C catalyst for methanol electrooxidation in acidic medium. *J Alloys Compd*. 2009;479:395-400.
- [13] Kang DK, Noh CS, Park ST, Sohn JM, Kim SK, Park YK. The effect of PtRuW ternary electrocatalysts on methanol oxidation reaction in direct methanol fuel cells. *Korean J Chem Eng*. 2010;27:802-806.
- [14] Chen W, Wei X, Zhang Y. A comparative study of tungsten-modified PtRu electrocatalysts for methanol oxidation. *Int J Hydrogen Energy*. 2014;39:6995-7003.
- [15] Philippe S, José LF. Carbon materials for catalysis. 2008, Wiley.
- [16] Radmilovic V, Gasteiger HA, Ross PN. Structure and chemical composition of a supported Pt-Ru electrocatalyst for methanol oxidation. *J Catal*. 1995;154:98-106.

- [17] Beyhan S, Leger JM, Kadirgan F. Pronounced synergetic effect of the nano-sized PtSnNi/C catalyst for ethanol oxidation in direct ethanol fuel cell. *Appl Catal B Environ.* 2013;130-131:305-313.
- [18] Priya M, Elumalai M, Arun A, Kiruthika S, Muthukumaran B. A development of ethanol/percarbonate membraneless fuel cells. *Advances in Physical Chemistry.* 2014;Article ID 862691:8.
- [19] Choi JH, Park KW, Park IS, Nam WH, Sung YE. Studies on the anode catalysts of carbon nanotube for DMFC. *Electrochimica Acta.* 2004;50:791-794.
- [20] Zhou Z, Wang S, Zhou W, Wang G, Jiang L, Li W. Novel synthesis of highly active Pt/C cathode electrocatalyst for direct methanol fuel cell. *Chem Commun.* 2003;394-395.
- [21] Bonesi AR, Moreno MS, Triaca WE, Luna AMC. Modified catalytic materials for ethanol oxidation. *Int J Hydrogen Energy.* 2010;35:5999-6004.
- [22] Vigier F, Coutanceau C, Hahn F, Belgsir EM, Lamy C. On the mechanism of ethanol electro-oxidation on Pt and PtSn catalysts: electrochemical and in situ IR reflectance spectroscopy studies. *J Electroanal Chem.* 2004;563:81-89.
- [23] Priya M, Elumalai M, Kiruthika S, Muthukumaran B. Influences of supporting materials for Pt-Ru binary catalyst in ethanol fuel cell. *Int J Mod Sci Technol.* 2016;1(1):5-11.
